Hindawi
Advances in Materials Science and Engineering
Volume 2022, Article ID 6009092, 10 pages
https://doi.org/10.1155/2022/6009092

Research Article

Defected Circular-Cross Stub Copper Metal Printed Pentaband Antenna

Anguraj Kandasamy,[1] **Saravanakumar Rengarasu**,[2] **Praveen Kitti Burri**,[3] **Satheeshkumar Palanisamy**,[4] **K. Kavin Kumar**,[5] **Aruna Devi Baladhandapani**,[6] **and Samson Alemayehu Mamo**[7]

[1]*Department of ECE, Sona College of Technology, Salem, Tamilnadu, India*
[2]*Department of Wireless Communication, Institute of ECE, Saveetha School of Engineering, Saveetha Institute of Medical and Technical Science, Chennai, Tamilnadu, India*
[3]*Department of ECE, PSCMR College of Engineering and Technology, Vijayawada, India*
[4]*Department of ECE, Coimbatore Institute of Technology, Coimbatore, Tamilnadu, India*
[5]*Department of ECE, Kongu Engineering College, Erode, Tamilnadu, India*
[6]*Department of ECE, Dr. N.G.P Institute of Technology, Dr. N.G.P. Nagar, Coimbatore, Tamil Nadu, India*
[7]*Department of Electrical and Computer Engineering, Faculty of Electrical and Biomedical Engineering, Institute of Technology, Hawassa University, Awasa, Ethiopia*

Correspondence should be addressed to Samson Alemayehu Mamo; samson@hu.edu.et

Received 8 January 2022; Accepted 23 April 2022; Published 19 May 2022

Academic Editor: V. Vijayan

A pentaband antenna is presented based on the conducting copper material printed on an FR4 substrate for the applications operating in the Gigahertz frequencies. The antenna has a substrate material with a dielectric constant of 4.4. The conducting copper is printed on the FR4 substrate acting as the radiating element and ground. The antenna radiating element has a defected circular structure with a cross stub. The proposed structure is operating at 2.64 GHz, 4.87 GHz, 7.86 GHz, 10.74 GHz, and 13.67 GHz. The antenna is simulated using CST software. The antenna is fabricated and validated with the measurement of return loss. The antenna simulated results like surface current distribution, gain, directivity, and radiation pattern prove that the proposed structure with its compact size is the right candidate for the GHz application.

1. Introduction

Many applications like medical and clinical imaging, sensing, and radar application widely use the GHz spectrum. In most communication devices, the space available for the antenna is minimal. So, there is a huge requirement for compact antennas, and also the multiband requirement is another major characteristic of the communication devices. The multiband antenna [1–16] can resonate at different bands, and hence it can be replaceable by multiple antennas operating at a different frequency. The microstrip patch antenna [1, 2] is the antenna currently used in the communication and GHz application due to its low profile. Another advantage is that it is the desirable antenna for multiband applications. There is a variety of techniques incorporated in the patch antenna to achieve multiband techniques. The techniques [3] include meandering of edges, parasitic patch elements, stacking of patches, a slot in the ground plane, and circular radiating elements [9–12]. However, all these make the structure complex, and it affects the antenna's performance. The metamaterial is the technique that researchers widely accept nowadays to achieve multiband characteristics.

Metamaterials [4, 5, 7, 11, 17–25] are artificial man-made structures that create a negative refractive index, improving antenna performance. The metamaterials are widely used in microstrip patch antennas to enhance gain and directivity, tune radiation characteristics, and achieve multiband [5, 6] characteristics. The metamaterial is an

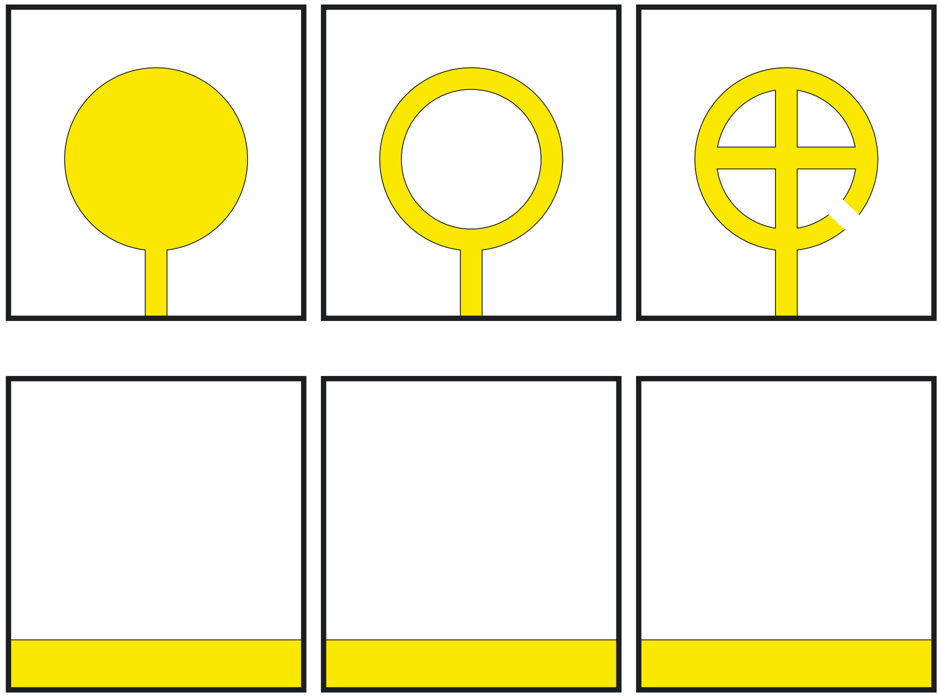

Figure 1: Step by step design of the C-shaped antenna with stub.

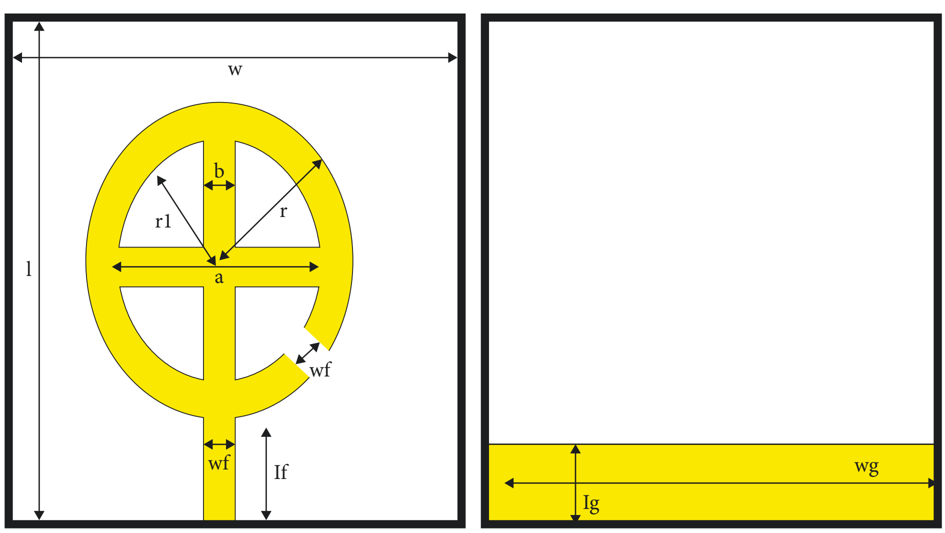

Figure 2: Pentaband cross stub circular monopole antenna.

artificial man-made structure with this property due to its periodic structure and not because of the chemical combinations available in the material. There are various types of metamaterial [26, 27] structures like split [28–34] and complementary split-ring resonators, anisotropic SRR-CSRR, broadside SRR-CSRR, omega, S, and Eight-shaped resonators.

This paper presents the defective circular antenna with cross stub for wireless application. In Section 2, the construction of the proposed structure is presented, and in Section 3, the parametric analysis is presented. In Section 4, the result is discussed, and the conclusion is presented in Section 5.

Table 1: Parameter value in mm.

w	l	Lg	A	b	wg
30	32	8	8	2	30
wf	lf	$r1$	R	h	t
2	10	7.74	10	1.6	0.035

2. C-Shaped Antenna with Cross Stub

In Figure 1, the step by step design procedure of the proposed C-shaped antenna with cross stub is presented. Figure 2 shows that the final proposed C-shaped antenna and its parameters are depicted, and the final parameter values are presented in Table 1.

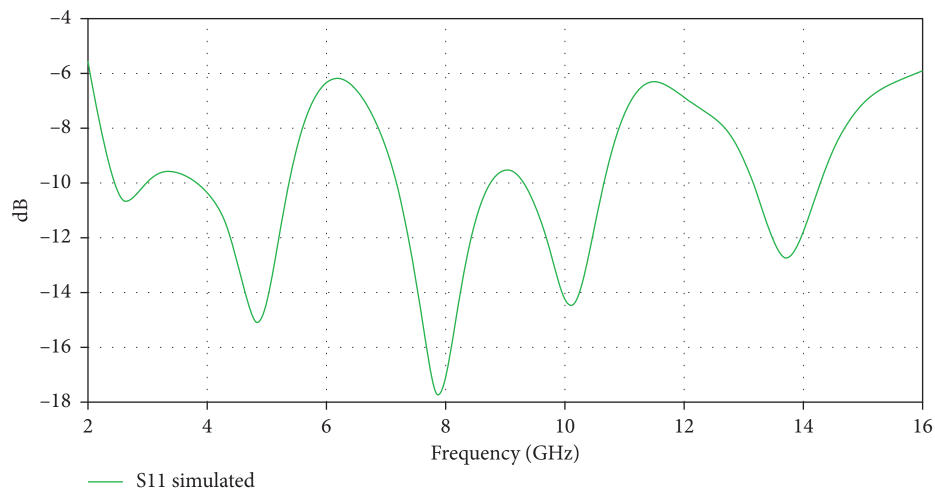

FIGURE 3: S_{11} simulated plot for pentaband cross stub circular monopole antenna.

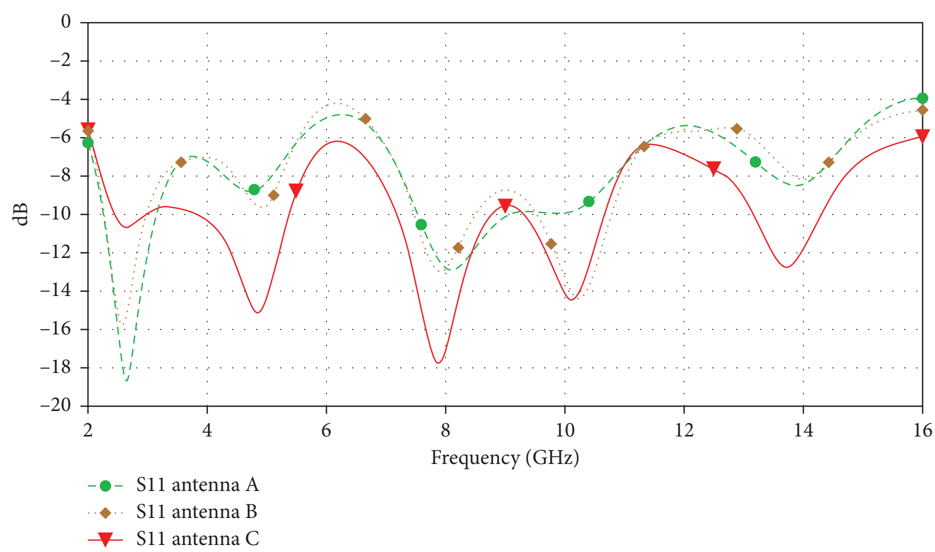

FIGURE 4: S_{11} comparision plot-various stages of pentaband cross stub circular monopole antenna.

Antenna A is a simple circular patch antenna with a radius of 10 mm, which resonates at a single band with an impedance bandwidth of 0.48 GHz. The resonant frequency of antenna A is 4.23 GHz. Then, antenna B is designed by including a circular slot of 7.74 mm, which is operating at dual-band at 4.21 GHz and 2.31 GHz. Antenna C is designed to create a slot in the circular radiating ring, and a cross-shaped stub is introduced, making the proposed C-shaped antenna with cross stub to operate at 4 different bands at 2.45, 4.51, 8.03, and 13.82 GHz. The resonating band of the antenna is from 2.12 GHz to 3.61 GHz with the return loss of −11.85 dB, from 3.98 GHz to 5.59 GHz with a return loss of −13.67 dB, from 7.12 GHz to 10.24 GHz with a return loss of −17.12 dB, and from 13.5 GHz to 14.32 GHz, with a return loss of −12.08 dB. The antenna's impedance bandwidth is 1.49 GHz, 1.61 GHz, 3.12 GHz, and 0.76 GHz in the respective bands. The proposed antenna's reflection coefficients are presented in Figure 3, from which we can observe that the proposed antenna has quad-band GHz resonance. In Figure 4, the comparison between the three evolution stages is presented.

3. Parametric Analysis of C-Shaped Antenna

The parametric analysis in CST identifies the correct value for the critical parameters. First, the slot radius $r1$ is chosen. It is varied from 7.74 mm to 9.74 mm in steps of 1 mm. The analysis of return loss concerning various slot radii is presented in Figure 4 ($r1 = 7.74$ mm is represented in red, $r1 = 8.74$ mm is represented green, and $r1 = 9.74$ mm is represented in blue). Figure 5 shows that as the slot's radius increases, the impedance bandwidth is very much reduced, and therefore 7.74 mm is chosen as the final value.

Then, the feed width is chosen for the parametric analysis, and it increased from 1 mm to 3 mm in steps of 1 mm. The feed width of 2 mm has good impedance matching and bandwidth in all the operating bands. Hence,

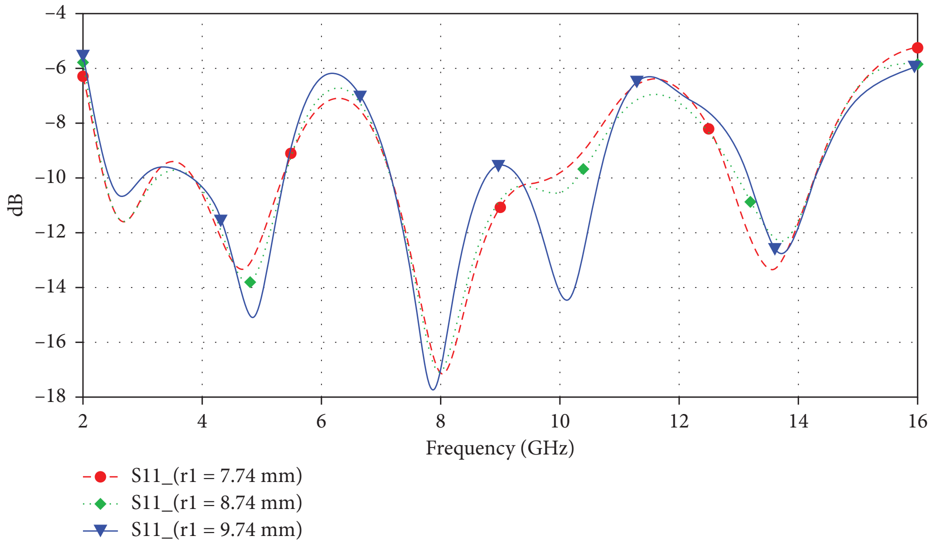

FIGURE 5: Parametric analysis-radius of the ring slot $r1$.

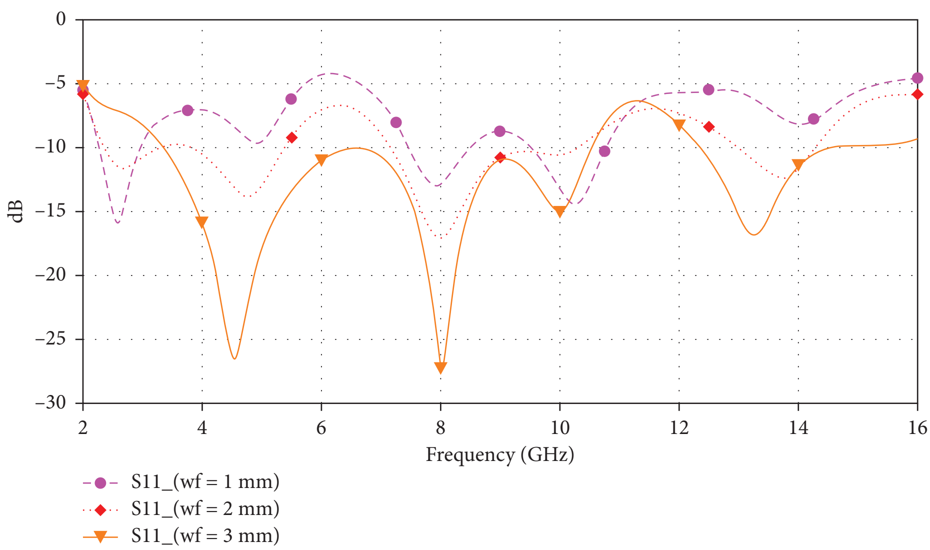

FIGURE 6: Parametric analysis-feed width wf.

it is chosen as the final value for the proposed C-shaped cross stub antenna. The effect of the feed with is presented in Figure 6 (wf = 1 mm is represented by pick colour, wf = 2 mm is represented by red colour, and wf = 3 mm is represented by orange colour) and followed by the ground length lg, which is changed from 6 mm to 8 mm in steps of 1 mm. And, it is noted that lg = 8 mm has good resonance behaviour in all the resonating bands, which is depicted in Figure 7 (lg = 6 mm is represented in yellow, lg = 7 mm is represented in red, and lg = 8 mm is represented in blue).

4. Result and Discussion

In Figure 8, the radiation pattern concerning various resonating frequencies is presented. From Figure 8, it is observed that the E plane has a perfect dipole pattern while the H plane has an omnidirectional pattern. The dipole and omnidirectional patterns are major requirements for any communication application.

In Figure 9, the surface current density at various resonating frequencies is presented, which depicts that the surface current is distributed evenly in the proposed structure over the entire operating frequency.

In Figure 10, the directivity is plotted for the resonant frequency; the maximum directivity is about 7.25 dBi. The directivity is above 2.5 dBi in all the resonating bands. The gain is also plotted with respect to the frequency in Figure 11. The maximum value of the gain is 6.25 dBi.

The proposed antenna is fabricated with the help of the photolithography method. The mask of the proposed antenna is placed on the FR4; before that the FR4 should be cleaned with the help of acetone. The substrate to be used should be double-side copper-clad FR4. Then, the Cu clad FR4 is UV exposed and immersed in NaCl developer solution. Then, etch

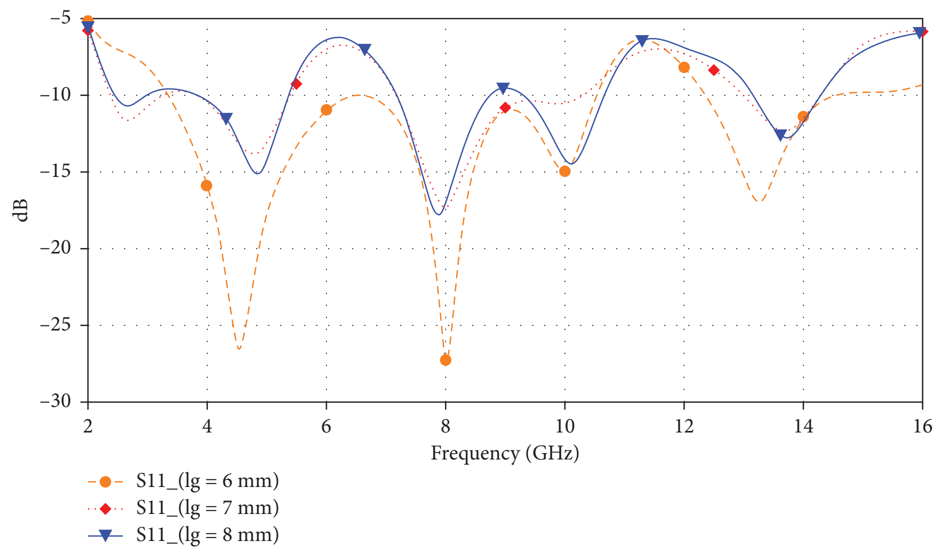

Figure 7: Parametric analysis-ground length lg.

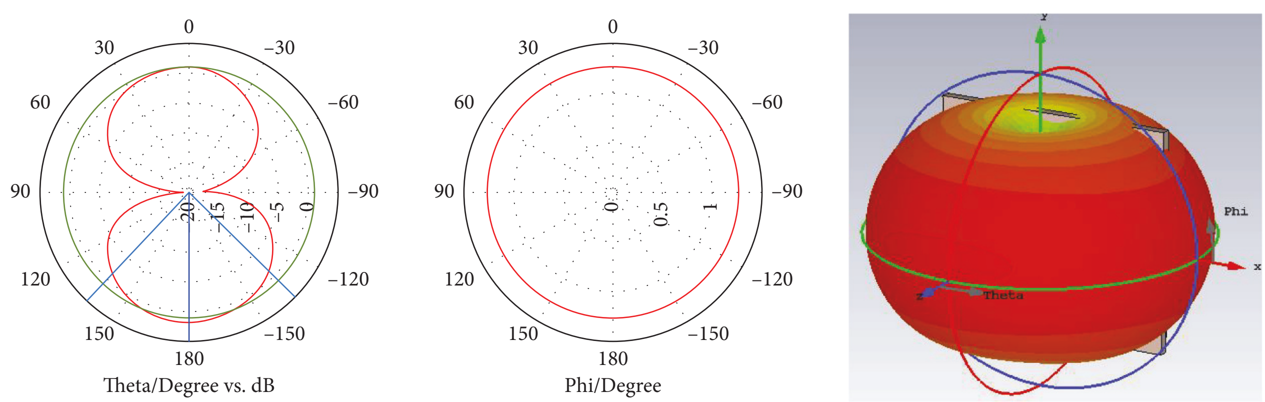

(a)

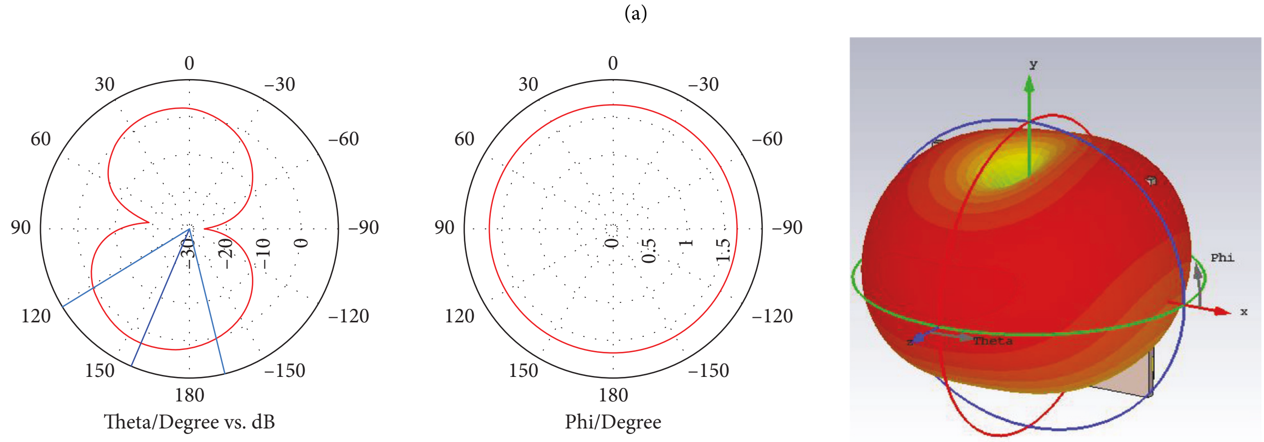

(b)

Figure 8: Continued.

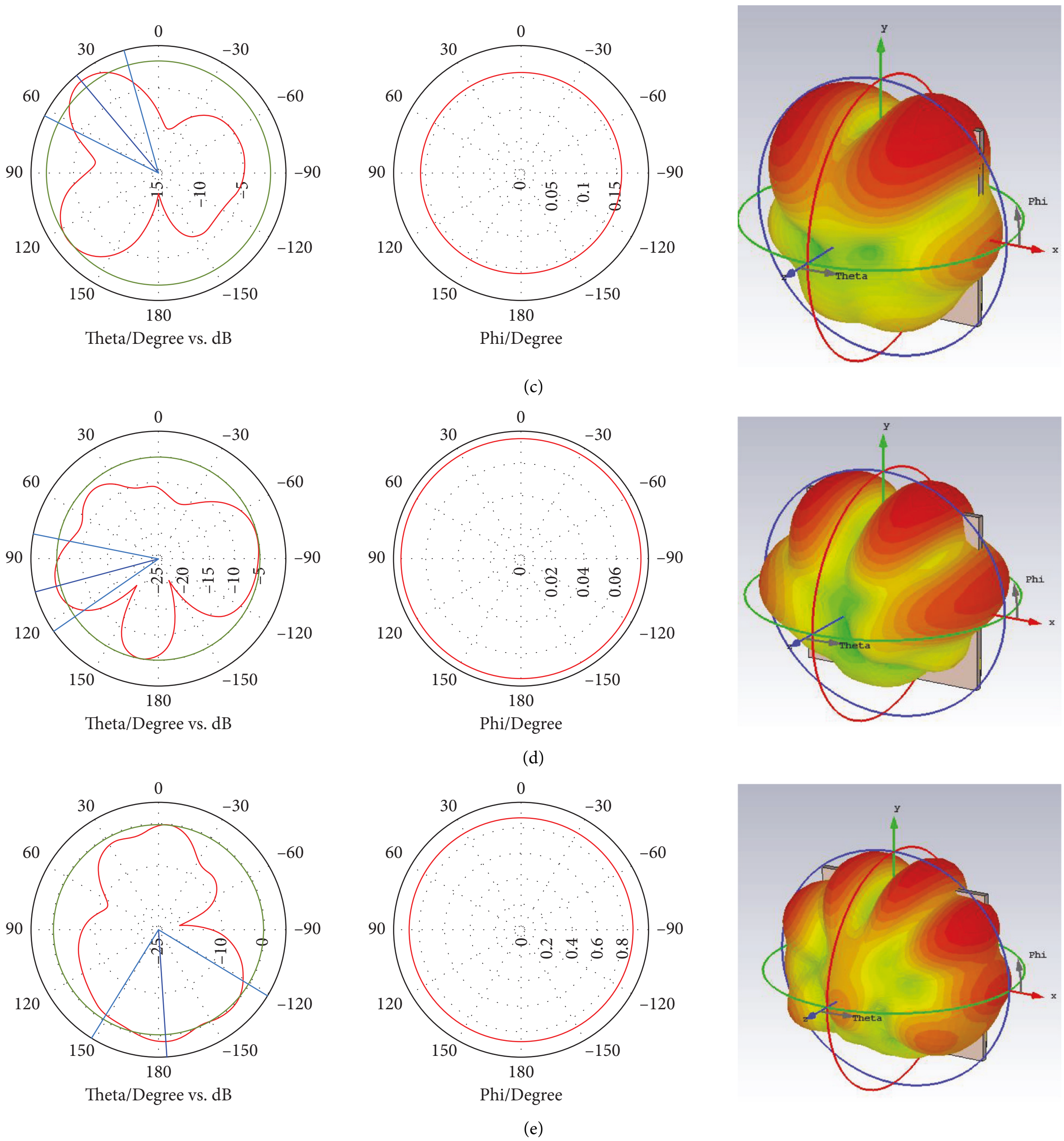

Figure 8: Radiation pattern at various resonating frequencies: (a) 2.64 GHz. (b) 4.87 GHz. (c) 7.86 GHz. (d) 10.74 GHz. (e) 13.67 GHz.

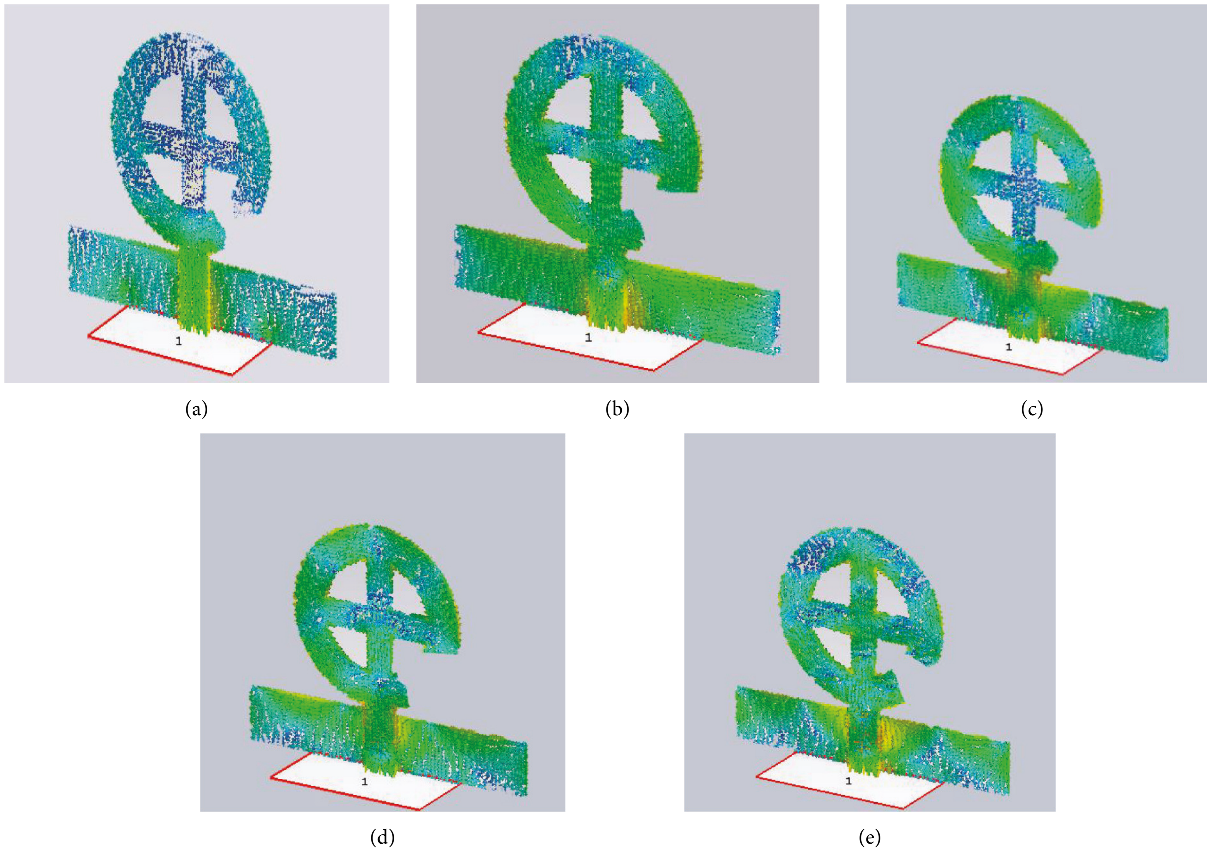

Figure 9: Distribution of surface current at various resonating frequencies: (a) 2.64 GHz. (b) 4.87 GHz. (c) 7.86 GHz. (d) 10.74 GHz. (e) 13.67 GHz.

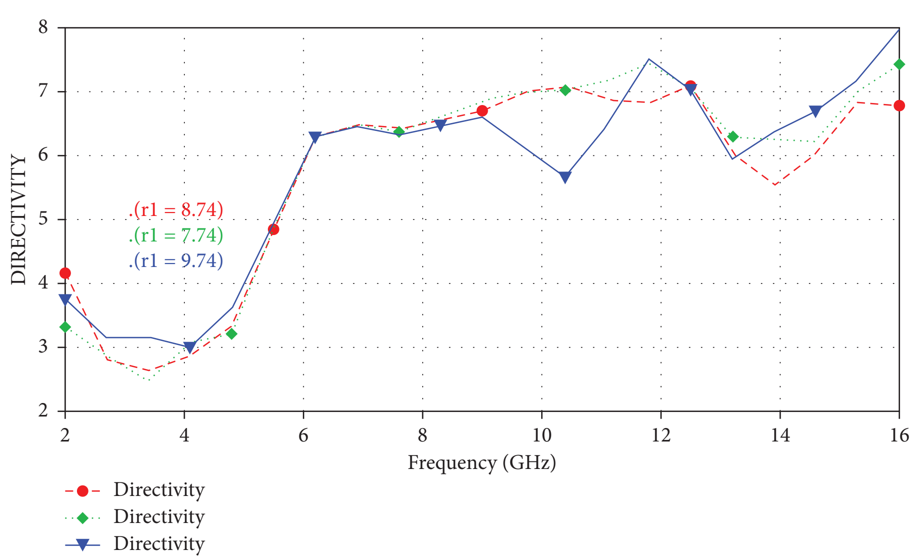

Figure 10: Directivity vs. frequency plot.

could be done with FeCl followed by a photoresist removal. The fabricated antenna with respect to the above procedure is presented in Figure 12. The proposed antenna is measured and compared with the simulated results in Figure 13. The deviation is due to the fabrication and measurement error.

In Figure 7, the directivity is plotted for the resonant frequency; the maximum directivity is about 7.25 dBi. The directivity is above 2.5 dBi in all the resonating bands. The gain is also plotted with respect to the frequency in Figure 8. The maximum value of the gain is 6.25 dBi.

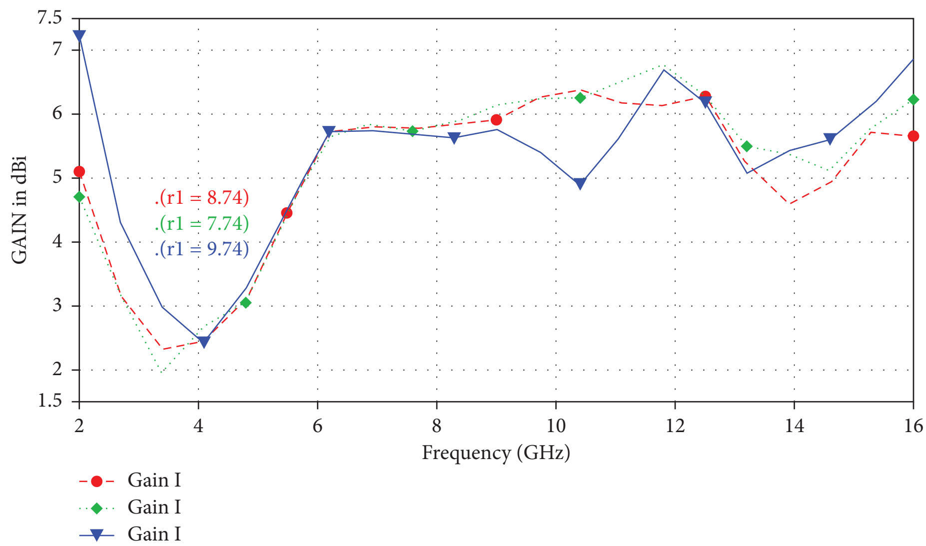

Figure 11: Gain vs. frequency plot.

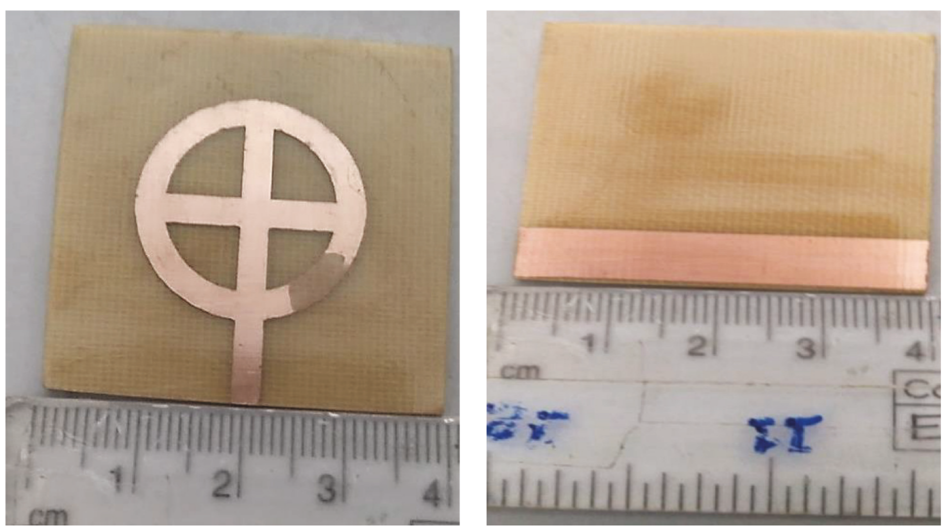

Figure 12: Fabricated antenna.

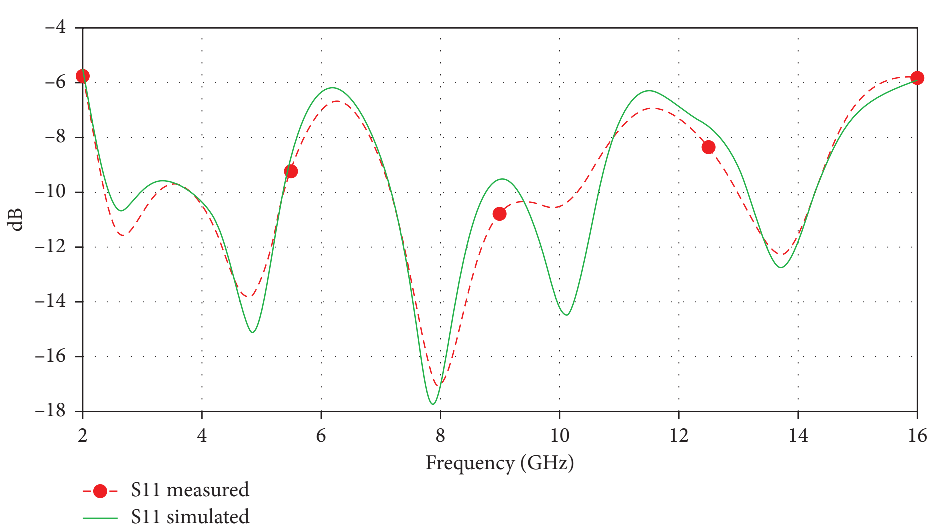

Figure 13: Simulated vs. measured S_{11} Plot.

5. Conclusion

A printed C-shaped patch with a cross stub is presented for the GHz application. The proposed structure has three stages of evolution. It is designed on an FR4 substrate with 30 mm × 32 mm × 1.6 mm. The antenna operates at 4 different bands at 2.45 GHz, 4.51 GHz, 8.03 GHz, and 13.82 GHz. The resonating band of the antenna is from 2.12 GHz to 3.61 GHz with the return loss of −11.85 dB, from 3.98 GHz to 5.59 GHz with a return loss of −13.67 dB, from 7.12 GHz to 10.24 GHz with a return loss of −17.12 dB, and from 13.5 GHz to 14.32 GHz, with a return loss of −12.08 dB. The antenna's impedance bandwidth is 1.49 GHz, 1.61 GHz, 3.12 GHz, and 0.76 GHz in the respective bands. The simulated result of the return loss, gain, directivity, E plane, and H plane radiation pattern is presented. The compact size, reasonable gain, and directivity with stable E plane and H plane radiation pattern make the proposed antenna to be the best choice for the proposed GHz application.

Data Availability

The data used to support the findings of this study are included in the article. Further data or information required are available from the corresponding author upon request.

Conflicts of Interest

The authors declare that there are no conflicts of interest regarding the publication of this paper.

Authors' Contributions

Dr. K. Anguraj, Dr. R. Saravanakumar, and B. Praveen Kitti performed study conception and design. S P Satheesh Kumar, K. Kavin kumar, and B. Aruna Devi were responsible for literature and data collection. P Satheesh Kumar, K. Kavin Kumar, Samson Alemayehu Mamo, and B. Aruna Devi were responsible for analysis, fabrication, and interpretation of results. Dr. R. Saravanakumar, B. Praveen Kitti, B. Aruna Devi, and P. Satheesh Kumar prepared the draft. Samson Alemayehu Mamo, B. Aruna Devi, and P. Satheesh Kumar validated the study. All authors reviewed the results and approved the final version of the manuscript.

References

[1] E. Lier and K. Jakobsen, "Rectangular microstrip patch antennas with infinite and finite ground plane dimensions," *IEEE Transactions on Antennas and Propagation*, vol. 31, no. 6, pp. 978–984, 1983.
[2] H. Zhu, S. W. Cheung, and T. I. Yuk, "Enhancing antenna boresight gain using a small metasurface lens reduction in half-power beamwidth," *IEEE Antennas and Propagation Magazine*, vol. 58, no. 1, pp. 35–44, 2016.
[3] A. Qureshi, M. U. Afzal, T. Tauqeer, and M. A. Tarar, "Performance analysis of FR-4 substrate for high-frequency microstrip antennas," in *Proceedings of the 2011 China-Japan Joint Microwave Conference*, Hangzhou, China, April 2011.
[4] C. Caloz and T. Itoh, *Electromagnetic Metamaterials: Transmission Line Theory and Microwave Applications*, Wiley-IEEE Press, New York, USA, 2005.
[5] A. Pirooj, M. Naser-Moghadasi, and F. B. Zarrabi, "Design of compact slot antenna based on split ring resonator for 2.45/5 GHz WLAN applications with circular polarization," *Microwave and Optical Technology Letters*, vol. 58, no. 1, pp. 12–16, 2016.
[6] D. H. Schaubert, D. M. Pozar, and A. Adrian, "Effect of microstrip antenna substrate thickness and permittivity: comparison of theories with experiment," *IEEE Transactions on Antennas and Propagation*, vol. 37, no. 6, pp. 677–682, 1989.
[7] G. Geetharamani and T. Aathmanesan, "Design of metamaterial antenna for 2.4 GHz WiFi applications," *Wireless Personal Communications*, vol. 113, no. 4, pp. 2289–2300, 2020.
[8] K. Scheuer, J. Holmes, E. Galyaev, D. Blyth, and R. Alarcon, "Radiation effects on FR4 printed circuit boards," *IEEE Transactions on Nuclear Science*, vol. 67, no. 8, pp. 1846–1851, 2020.
[9] K. Wei, B. Zhu, and M. Tao, "The circular polarization diversity antennas achieved by a fractal defected ground structure," *IEEE Access*, vol. 7, pp. 92030–92036, 2019.
[10] K. Wei, J. Y. Li, L. Wang, R. Xu, and Z. J. Xing, "A new technique to design circularly polarized microstrip antenna by fractal defected ground structure," *IEEE Transactions on Antennas and Propagation*, vol. 65, no. 7, pp. 3721–3725, 2017.
[11] S. P. J. Christydass and N. Gunavathi, *Design of CSRR Loaded Multiband Slotted Rectangular Patch Antenna*, in *Proceedings of the 2017 IEEE Applied Electromagnetics Conference (AEMC)*, pp. 1-2, Aurangabad, India, December 2017.
[12] R. Boopathi Rani and S. K. Pandey, "A CPW-fed circular patch antenna inspired by reduced ground plane and CSRR slot for UWB applications with notch band," *Microwave and Optical Technology Letters*, vol. 59, no. 4, pp. 745–749, 2017.
[13] F. J. Herraiz-Martinez, G. Zamora, F. Paredes, F. Martin, and J. Bonache, "Multiband printed monopole antennas loaded with OCSRRs for PANs and WLANs," *IEEE Antennas and Wireless Propagation Letters*, vol. 10, pp. 1528–1531, 2011.
[14] P. Pingan Liu, Y. Yanlin Zou, B. Baorong Xie, X. Xianglong Liu, and B. Baohua Sun, "Compact CPW-fed tri-band printed antenna with meandering split-ring slot for WLAN/WiMAX applications," *IEEE Antennas and Wireless Propagation Letters*, vol. 11, pp. 1242–1244, 2012.
[15] A. T. Abed and A. M. Jawad, "Compact size MIMO amer fractal slot antenna for 3G, LTE (4G), WLAN, WiMAX, ISM and 5G communications," *IEEE Access*, vol. 7, pp. 125542–125551, 2019.
[16] S. S. Al-Bawri, S. Islam, H. Y. Wong, and M. F. Jamlos, "Bandwidth and gain enhancement of quad-band CPW-fed antenna for wireless applications," *Sensors*, vol. 20, no. 2, 2020.
[17] G. Dattatreya and K. K. Naik, "A low volume flexible CPW-fed elliptical-ring with split-triangular patch dual-band antenna," *International Journal of RF and Microwave Computer-Aided Engineering*, vol. 29, no. 8, 2019.
[18] A. Balanis, *Antenna Theory-Analysis and Design*, Wiley, Hoboken, NJ, USA, 3rd edition, 2005.
[19] K. N. Paracha, S. K. A. Rahim, H. T. Chattha, S. S. Aljaafreh, S. u. Rehman, and Y. C. Lo, "Low-cost printed flexible antenna by using an office printer for conformal applications," *International Journal of Antennas and Propagation*, vol. 2018, pp. 1–7, 2018.

[20] S. P. J. Christydass, J. Suganthi, S. Kavitha, and R. Yuvaraj, “Ring monopole antenna for Tera-Hertz application,” *Materials Today Proceedings*, vol. 45, pp. 1827–1833, 2021.

[21] A. Moradhesari, M. Naser-Moghadasi, and F. G. Gharakhili, “Design of compact CPW-fed monopole antenna for WLAN/ WiMAX applications using a pair of F-shaped slits on the patch,” *Microwave and Optical Technology Letters*, vol. 55, no. 10, pp. 2337–2340, 2013.

[22] W. A. G. Al-Tumah and R. M. Shaaban, “Akeel Tahir, “Design, simulation and measurement of triple band annular ring microstrip antenna based on shape of crescent moon,” *AEU - International Journal of Electronics and Communications*, vol. 117, 2020.

[23] C. Elavarasi and T. Shanmuganantham, “Multiband SRR loaded leaf-shaped Koch fractal with a modified CPW-fed antenna,” *International Journal of Electronics Letters*, vol. 6, no. 2, pp. 137–145, 2017.

[24] A. Iqbal, A. Bouazizi, O. A. Saraereh, A. Basir, and R. K. Gangwar, “Design of multiple band, meandered strips connected patch antenna,” *Progress In Electromagnetics Research Letters*, vol. 79, pp. 51–57, 2018.

[25] P. Ciais, R. Staraj, G. Kossiavas, and C. Luxey, “Compact internal multiband antenna for mobile phone and WLAN standards,” *Electronics Letters*, vol. 40, no. 15, p. 920, 2004.

[26] S. Prasad Jones Christydass and N. Gunavathi, “Octa-band metamaterial inspired multiband monopole antenna for wireless application,” *Progress In Electromagnetics Research C*, vol. 113, pp. 97–110, 2021.

[27] J. Liang and H. Y. D. Yang, “Varactor loaded tunable printed PIFA,” *Progress In Electromagnetics Research B*, vol. 15, pp. 113–131, 2009.

[28] J.-L. Jaw and J.-K. Chen, “CPW-fed hook-shaped strip antenna for dual wideband operation,” *Journal of Electromagnetic Waves and Applications*, vol. 22, no. 13, pp. 1809–1818, 2008.

[29] S. Prasad Jones Christydass and N. Gunavathi, “Dual-band complementary split-ring resonator engraved rectangular monopole for gsm and wlan/wimax/5G sub-6 Ghz band (new radio band),” *Progress In Electromagnetics Research C*, vol. 113, pp. 251–263, 2021.

[30] A. K. Gautam, L. Kumar, B. K. Kanaujia, and K. Rambabu, “Design of compact F-shaped slot triple-band antenna for WLAN/WiMAX applications,” *IEEE Transactions on Antennas and Propagation*, vol. 64, no. 3, pp. 1101–1105, 2016.

[31] P. J. C Sam and N. Gunavathi, “A tri-band monopole antenna loaded with circular electric-inductive-capacitive metamaterial resonator for wireless application,” *Applied Physics A*, vol. 126, no. 10, pp. 774–811, 2020.

[32] Q. H. Sultan and A. M. A. Sabaawi, “Design and implementation of improved fractal loop antennas for passive UHF RFID tags based on expanding the enclosed area,” *Progress In Electromagnetics Research C*, vol. 111, pp. 135–145, 2021.

[33] S. M. Shamim, M. S. M. R. Uddin, and M. Samad, “Design and implementation of miniaturized wideband microstrip patch antenna for high-speed terahertz applications,” *Journal of Computational Electronics*, vol. 20, no. 1, pp. 604–610, 2021.

[34] G. Krishnaveni and B. Manimegalai, “Efficient and optimized design of a stacked patch microstrip antenna for next generation network applications,” *Journal of Ambient Intelligence and Humanized Computing*, vol. 12, no. 3, pp. 4093–4099, 2021.